Examination of Possibly Induced Seismicity from Hydraulic Fracturing in the Eola Field, Garvin County, Oklahoma

Austin Holland

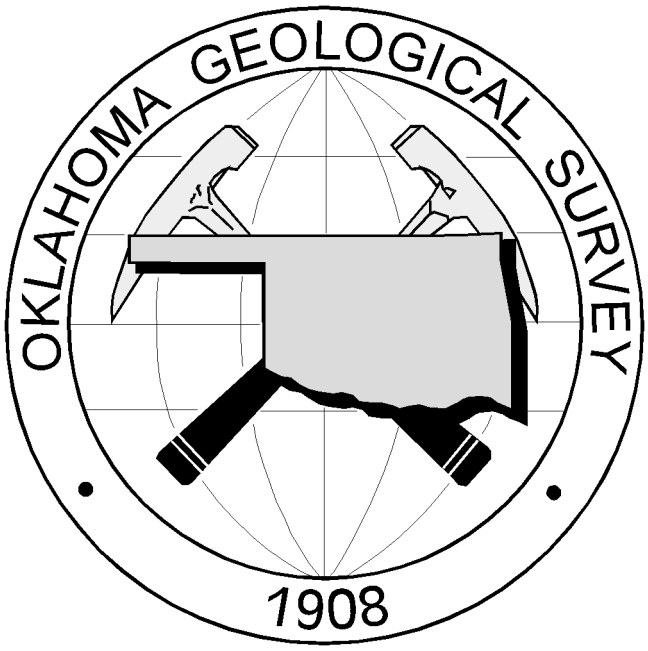

Oklahoma Geological Survey
Open-File Report
OF1-2011

OKLAHOMA GEOLOGICAL SURVEY
Open-file Report Disclaimer

This Open-file Report is intended to make the results of research available at the earliest possible date and not intended to represent the final or formal publication. The report is an unedited copy prepared by the author.

Examination of Possibly Induced Seismicity from Hydraulic Fracturing in the Eola Field, Garvin County, Oklahoma

Austin A. Holland
Oklahoma Geological Survey
Sarkeys Energy Center
100 East Boyd St., Rm. N-131
Norman, Oklahoma 73019-0628

August 2011

Oklahoma Geological Survey
Open-File Report
OF1-2011

Summary

On January 18, 2011, The Oklahoma Geological Survey (OGS) received a phone call from a resident living south of Elmore City, in Garvin County, Oklahoma, that reported feeling several earthquakes throughout the night. The reporting local resident had also offered that there was an active hydraulic fracturing project occurring nearby. Upon examination there were nearly 50 earthquakes, which occurred during that time. After analyzing the data there were 43 earthquakes large enough to be located, which from the character of the seismic recordings indicate that they are both shallow and unique. The earthquakes range in magnitude from 1.0 to 2.8 Md and the majority of earthquakes occurred within about 24 hours of the first earthquake. Careful attention and significant effort was put into obtaining the most accurate locations possible and gaining a reasonable estimate in the error in locations. The nearest seismic station is 35 km away from where the earthquakes occurred. Formal errors in location are on the order 100-500 m horizontally and about twice that for depth. Examination of different velocity models would suggest that the uncertainties in earthquake locations should be about twice the formal uncertainties. The majority of earthquakes appear to have occurred within about 3.5 km of the well located in the Eola Field of southern Garvin County. The Eola Field has many structures, which may provide conduits for fluid flow at depth. The well is Picket Unit B well 4-18, and about seven hours after the first and deepest hydraulic fracturing stage started the earthquakes began occurring. It was possible to model 95% of the earthquakes in this sequence using a simple pore pressure diffusion model with a permeability of about 250 mD (milliDarcies). While this permeability may be high it is less than those reported for highly fractured rock. The strong correlation in time and space as well as a reasonable fit to a physical model suggest that there is a possibility these earthquakes were induced by hydraulic-fracturing. However, the uncertainties in the data make it impossible to say with a high degree of certainty whether or not these earthquakes were triggered by natural means or by the nearby hydraulic-fracturing operation.

Introduction

On January 18th, 2011, a resident living in south-central Oklahoma (Garvin County), living south of Elmore City contacted the Oklahoma Geological Survey (OGS) to report feeling several earthquakes throughout the night with the first occurring at approximately 6:10 PM CST Jan. 17th and another large one at about 2:50 AM CST Jan. 18th. Upon examination there were in fact earthquakes in the area. The resident also reported that there was an active hydraulic fracturing project being conducted in a nearby well. Examination of the available seismic data, including EarthScope USArray stations in the region, quickly confirmed that earthquakes were occurring in the area. At this point the OGS contacted the Regional Manager for the Oklahoma Corporation Commission, who indicated that there was indeed fracturing occurring at the Picket Unit B Well 4-18. Our analysis showed that shortly after hydraulic fracturing began small earthquakes started occurring, and more than 50 were identified, of which 43 were large enough to be located. Most of these earthquakes

occurred within a 24-hour period after hydraulic fracturing operations had ceased. There have been previous cases where seismologists have suggested a link between hydraulic fracturing and earthquakes, but data was limited, so drawing a definitive conclusions was not possible for these cases. The first case occurred in June1978 in Carter and Love Counties, just south of Garvin County, with 70 earthquakes in 6.2 hours. The second case occurred in Love County with 90 earthquakes following the first and second hydraulic fracturing stages (Nicholson and Wesson, 1990).

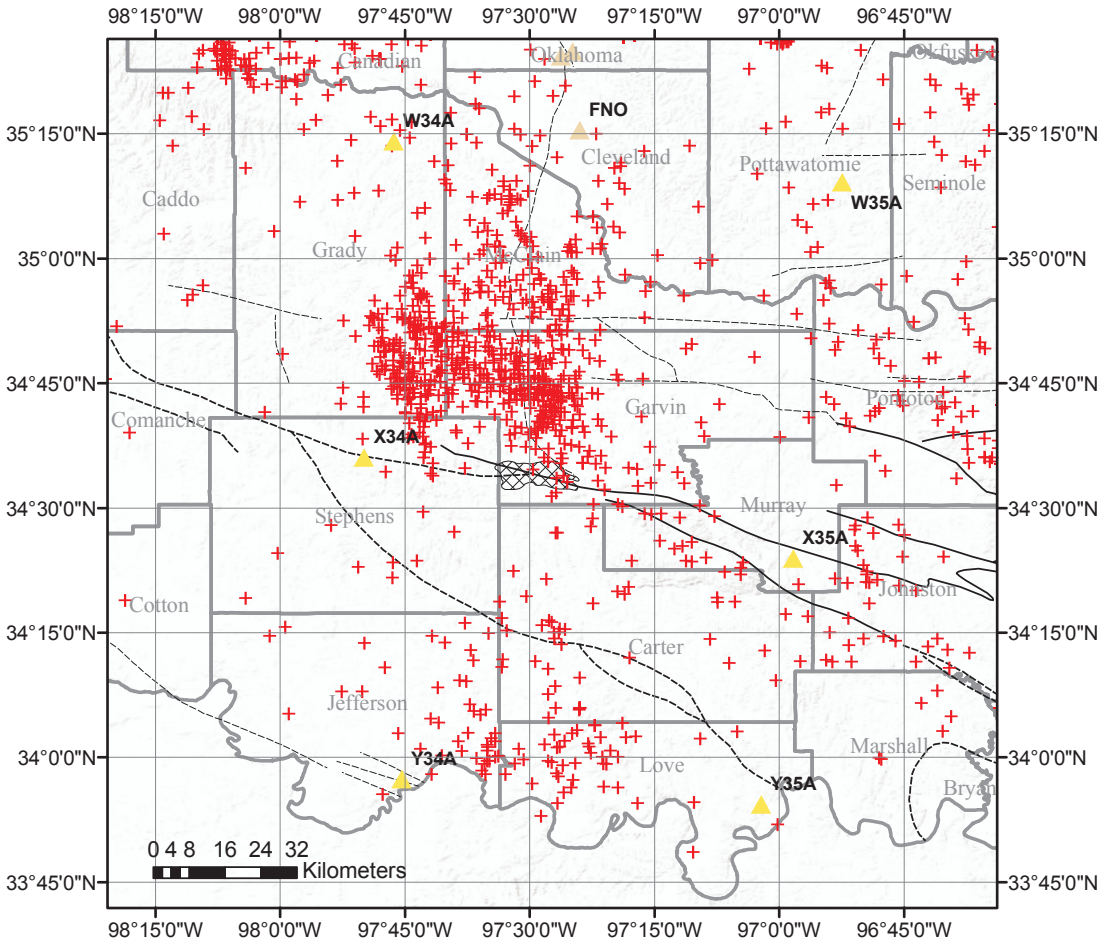

Figure 1 - Earthquakes from 1897-2010 from the OGS catalog (red crosses). Yellow triangles are seismic stations from the Earthscope Transportable Array; tan triangles are OGS seismic stations. Faults are shown by thin black lines, solid are faults mapped from a surface expression, dotted lines indicate subsurface faults (Northcutt and Campbell, 1995). The main movement on all of these faults was in the Pennsylvanian (Granath, 1989). Hachured region shows the location of the Eola Oil Field (Boyd, 2002).

South-central Oklahoma has a significant amount of historical seismicity, and has been one of the most active areas within Oklahoma since 1977, when an adequate seismic network was established. The nearest stations to the earthquakes were several Earthscope Transportable Array (TA) stations. Without the TA stations only

a few of the earthquakes could possibly have been located and the uncertainties in the hypocentral locations would be quite large.

Geologic Setting

The Eola Field lies at the northern edge of the Ardmore Basin and the buried northwestern extent of the Arbuckle Mountains and contains a highly folded and faulted thrust system (Swesnick and Green, 1950; Harlton, 1964, Granath, 1989). In the Cambrian this area experienced significant rifting associated with the Southern Oklahoma aulacogen (Keller et al., 1983). After the initial rifting the area experienced thermal subsidence and sedimentation (Granath, 1989). The area continued to see periods of subsidence and sedimentation with a few periods of erosion represented by unconformities (Swesnik and Green, 1950). In the mid-Pennsylvanian the area began to experience significant transpression associated with the Ouachita Orogen (Granath, 1989). Because of the areas complex tectonic history it is quite likely that the nature of faults has changed through time and that normal faults associated with the aulacogen and later basin accommodation were reactivated in the mid to late-Pennsylvanian with a new sense of motion. The Washita Valley fault is the largest fault in the area, with a surface trace of approximately 56 km (Tanner, 1967). It is a major fault that is known to extend nearly 180 km from the Ouachita thrust system in the southeast to the Anadarko basin to the northwest (Tanner, 1967). Estimates for the amount of left-lateral strike-slip accommodated on this fault vary dramatically, but reasonably range from 65 km (Tanner, 1967) to 26 km (McCaskill, 1998). The Roberson fault, to south of the Washita Valley fault, is a thrust fault with an associated overturned syncline with significant shortening (Swesnick and Green, 1950). The Reagan, Eola and Mill Creek faults as mapped by Harlton (1964) all show significant components of left lateral strike slip (Granath, 1989). The Eola field contains several fault blocks in between these major faults, with all the faults in the subsurface having near vertical dips (Harlton, 1964). To the southeast of the Eola Field is the highly faulted West Timbered Hills of the northwestern Arbuckle Mountains (Harlton, 1964).

The Eola Field was discovered in 1947 with a discovery well completed to a total depth of 10,234 feet (3,119 m) in the basal Bromide Sandstone. The initial bottom hole pressure was about 3800 PSI and by 1950 had declined to 2,900 PSI with seven producing wells in the field (Swesnick and Green, 1950).

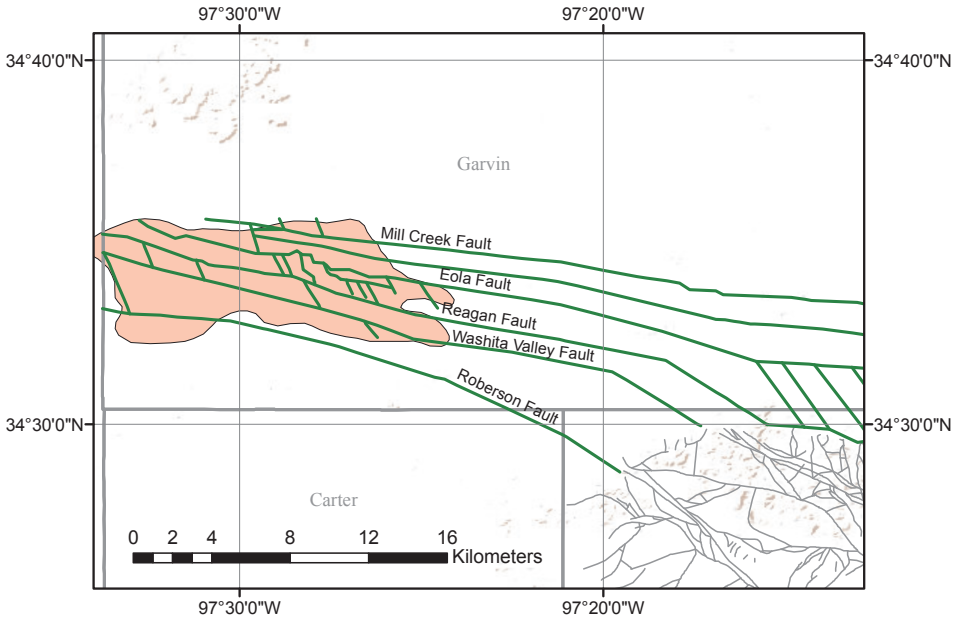

Figure 2 - Fault map for the Eola Field, Oklahoma. Thick green lines are faults modified from Harlton (1964). Faults shown as thin grey lines are from Stoeser et al. (2007). Eola field is colored a salmon color (Boyd, 2002).

Hydraulic Fracturing Operations at Picket Unit B Well 4-18

Hydraulic fracturing operations began on Monday January 17, 2011 at approximately 6 AM (CST), 12:00 UTC. The hydraulic fracturing of the well consisted of a four-stage hydraulic fracturing operation with frac intervals of 9,830'-10,282', 8,890'-8326', 7,662'-8,128', and 7,000'-7,562', with the last frac stage completed on January 23, 2011. The well was then flushed until February 6, 2011. Because the earthquakes began after the first frac stage we will primarily consider this stage. The first frac stage had an average rate of injection of 88.5 bpm and an average injection pressure of 4850 psi. This stage also included an acid stimulation. There was a total of 2,475,545 gallons of frac fluid injected and 575,974 lbs of propent. The Picket Unit B well 4-18 is a nearly vertical well located at 34.55272 -97.44580, elevation 277.4 m, with an API number of 049-24797. The first frac occurred in the interval beteween 9,830' (2,996.2 m), and 10,282' (3,134.0 m)

Earthquake Data Analysis and Methods

The Garvin County, earthquakes were analyzed using routine processing steps by the OGS for earthquake monitoring. The phase arrivals were picked using the interactive picking capabilities of the seismic software package SEISAN (Havskov and Ottemoller, 1999). The earthquake hypocenters and origin times were determined using the location program HYPOCENTER (Lienert et al., 1986 and Lienert and Havskov, 1995). The OGS typical duration magnitude calculations were

used to determine the magnitude of the earthquakes (Lawson and Luza, 2006). The velocity model used is the same model that is currently being used by the OGS for most regions of Oklahoma, the "Manitou Model" shown in Table 1. Using the HYPOELLIPSE method hypocenter locations are poorly resolved because the nearest station is approximately 35 km away, phase arrivals were difficult to identify for these events, and the events appear to have been shallow. The formal uncertainties are significant in the range of several kilometers for these earthquakes and indicate that locations for these earthquakes should be considered suspect. The formal error estimates from the initial HYPOCENTER locations can be seen in Table 2. Aside from the formal uncertainties it is very likely that the regional velocity model used is not quite appropriate for this area of Oklahoma. In fact, a single velocity model is definitely not appropriate across the structurally complex region spanning the deep (>10km) Ardmore basin to the immediately adjacent Arbuckle uplift.

In an attempt to improve the hypocenter determinations the Double-Differencing, HypoDD, technique of Waldhauser and Ellsworth (2000) was employed to relocate the earthquakes. This approach takes advantage of the fact that there is very little difference in phase traveltimes between earthquakes that occur near each other. It can then use all the earthquakes to find the centroid of the earthquakes, while more easily identifying and excluding bad phase arrival times at stations. Once the centroid of the earthquakes is determined the relative location of each earthquake to the centroid can accurately be determined. HypoDD provides very good resolution of relative earthquake locations, but the absolute earthquake location error can be larger than the formal error estimates. The singular value decomposition (SVD) method was used in HypoDD because this is a small dataset, and the SVD method provides a better estimate of the formal uncertainties (Waldhauser, 2001).

HypoDD also has the capability to use waveform cross correlation between events. Waveform cross-correlations can often dramatically improve earthquake hypocentral location errors, by removing any human error in phase arrival picks. This method uses the similarities in waveforms between events to more accurately measure arrival times, and has been shown to dramatically improve locations and their associated uncertainties. Cross correlation is simply finding the part of the recorded waveform, which is most like the template waveform window. A template waveform window is an example waveform around either a P or S-Wave arrival from an event within the earthquake sequence. Cross correlations for these earthquakes were attempted. In order to attempt the cross correlation a few of the larger events were selected as templates and windows around the P and S phase arrivals were selected. These windows where then run against the corresponding template event to determine how well the data could be cross-correlated with the entire waveform for the respective earthquake. In this test, the S-waves could readily be identified using cross correlation, but the P-wave could not. The P-waves were generally correlating better with S or surface waves in the coda than with the P phase arrival, except for two stations X34A and Y34A. The inability to cross-

Table 1 - Velocity models used in this study; all have a Vp/Vs ratio of 1.73. Manitou and Chelsea models are derived from Mitchell and Landisman (1970). Tryggvason and Qualls (1967) model was developed from the same seismic refraction line as Mitchell and Landisman (1970). The Central Oklahoma model was developed from traveltime inversion for earthquakes in central Oklahoma.

Chelsea			Central Oklahoma		
Thickness (km)	Vp (km/s)	Vs (km/s)	Thickness (km)	Vp (km/s)	Vs (km/s)
0.6	4.00	2.31	0.5	4.46	2.58
0.4	6.05	3.50	0.5	4.60	2.66
2.1	5.50	3.18	2.0	4.75	2.75
10.3	6.08	3.51	0.5	6.13	3.54
3.0	6.49	3.75	1.5	6.16	3.56
1.5	6.20	3.58	3.0	6.19	3.58
8.2	6.72	3.88	2.0	6.19	3.58
9.1	7.05	4.08	5.0	6.20	3.58
11.1	7.36	4.25	11.0	6.73	3.89
half-space	8.18	4.73	9.0	7.10	4.11
			11.0	7.36	4.25
			half-space	8.18	4.73

Manitou			Tryggvason-Qualls		
Thickness (km)	Vp (km/s)	Vs (km/s)	Thickness (km)	Vp (km/s)	Vs (km/s)
1.0	5.50	3.18	0.54	4.00	2.31
9.5	6.08	3.51	13.16	5.96	3.45
5.1	6.49	3.75	15.90	6.66	3.85
2.5	6.20	3.58	21.84	7.20	4.16
8.2	6.72	3.88	half-space	8.32	4.81
9.1	7.05	4.08			
11.1	7.36	4.25			
half-space	8.18	4.73			

Table 2 – Initial hypocenter locations from SEISAN and HYPOCENTER. Large uncertainties in hypocentral locations are typical of earthquakes without nearby seismic stations. The mean error at a 90% confidence interval in locations is 3.8, 5.2, 14.4 km for longitude, latitude, depth respectively.

Origin Time	Longitude	Latitude	Depth (km)	Magnitude	Type	RMS	Error Longitude (km)	Error Latitude (km)	Error Depth (km)
1/17/11 19:19	-97.4238	34.5285	8.2	1.3	Md	0.61	4.1	11.5	16.7
1/17/11 19:35	-97.4488	34.5583	3	1.9	Md	1.04	3.8	3.8	0
1/17/11 20:04	-97.4418	34.5525	0	1.5	Md	0.99	4.9	8	24.2
1/17/11 20:16	-97.4274	34.5585	1	2.1	Md	0.79	2.7	2.6	0
1/17/11 20:50	-97.4199	34.5487	5	1.6	Md	0.64	4.4	6.3	17.3
1/17/11 20:56	-97.4318	34.5637	0	2.1	Md	0.99	3.3	3.3	10.4
1/17/11 21:12	-97.4391	34.5738	0.1	1.8	Md	0.95	4.2	4.8	19.7
1/17/11 21:23	-97.4051	34.5587	0	1.7	Md	1.31	5	7.1	18.6
1/17/11 21:44	-97.41	34.5439	0	1.6	Md	0.49	3.5	6.9	18.5
1/17/11 21:46	-97.4239	34.561	0	2	Md	0.8	3.3	4.8	13
1/17/11 22:27	-97.4076	34.5592	0	2.2	Md	0.67	2.6	4.4	9.9
1/17/11 22:35	-97.4311	34.5521	0	2.3	Md	0.89	3	3.1	9.7
1/17/11 23:24	-97.4041	34.569	0	1.7	Md	0.8	4.9	5.7	26.4
1/17/11 23:37	-97.4304	34.5784	0	1.6	Md	0.96	4.9	5.9	24.3
1/17/11 23:48	-97.4113	34.5474	0	1.9	Md	0.82	2.8	3.4	9.2
1/17/11 23:52	-97.4247	34.5263	0	1.4	Md	0.26	2.7	4.7	16.1
1/18/11 0:14	-97.433	34.5597	0	2.6	Md	0.77	2.4	2.8	8.1
1/18/11 0:33	-97.4048	34.5463	0	1.7	Md	0.51	3	3.4	14.4
1/18/11 0:34	-97.413	34.5352	0	1.3	Md	0.65	4.2	5.6	16.4
1/18/11 0:46	-97.4173	34.5142	0	1	Md	0.41	3	5	16.4
1/18/11 1:05	-97.4363	34.5644	0	1.6	Md	0.77	3.1	3.6	12.7
1/18/11 1:06	-97.4164	34.5146	0	1.2	Md	0.56	3.4	6.2	14.4
1/18/11 1:31	-97.438	34.5619	0	1.7	Md	1.06	4.9	5	20.4
1/18/11 1:37	-97.4277	34.5368	5	1.7	Md	0.81	4.7	10.2	18.5
1/18/11 1:40	-97.4424	34.5679	0.1	2.2	Md	0.93	3.4	4.2	12.1
1/18/11 2:13	-97.4347	34.5653	0	2	Md	0.95	3.6	4.2	15.9
1/18/11 2:27	-97.4077	34.5587	4.7	1.5	Md	0.43	3.1	7.9	12.3
1/18/11 2:43	-97.4496	34.5659	0	2	Md	1.01	3.9	4.8	16
1/18/11 3:17	-97.4502	34.5838	0	1.8	Md	1.01	4.7	5.2	16.7
1/18/11 3:40	-97.43	34.5663	0	2.8	Md	1.17	3.2	3.7	8.7
1/18/11 4:01	-97.419	34.5466	0	2.4	Md	0.96	2.7	3.6	8.6
1/18/11 4:52	-97.3959	34.5516	0	1.5	Md	0.83	4.5	6.5	17.2
1/18/11 5:57	-97.4264	34.5481	0	2.1	Md	0.62	2.3	3.4	10.6
1/18/11 7:05	-97.4383	34.5633	0	1.2	Md	0.94	4.3	6.5	23.2
1/18/11 7:58	-97.4009	34.5375	0	1.2	Md	1.34	6.8	9.4	23.2
1/18/11 7:59	-97.4195	34.5341	8.2	1.3	Md	0.45	3.2	6.3	8
1/18/11 8:23	-97.4227	34.562	0	1.7	Md	1.15	4	6	13.3
1/18/11 9:22	-97.4302	34.5572	0.1	2.3	Md	0.68	2.6	3.9	9.6
1/18/11 9:52	-97.4188	34.5326	0	1.5	Md	0.63	3.2	5	13.9
1/18/11 12:32	-97.4296	34.5685	0	2	Md	1.06	3.7	4.7	13.2
1/18/11 12:43	-97.4106	34.5279	0	1.5	Md	1.03	7.9	10.5	22.5
1/18/11 19:40	-97.4247	34.5382	0	1.4	Md	0.5	2.6	4.1	18.3
1/19/11 4:29	-97.4259	34.5555	0.1	2	Md	0.82	4.4	3.9	13

correlate an earthquake's P-Wave arrival with the template, excluded the possibility of using cross-correlation data for earthquake relocations using HypoDD.

Because the events are shallow, the hypocentral depths were fixed to 2.5 km to prevent events that were initially located at the surface from being excluded immediately in the relocation process. In order to address the sensitivity to velocity models, relocations were conducted for all velocity models listed in Table 1. Only the velocity model varied between HypoDD relocations for the different velocity models. These models all correspond reasonably well and earthquakes hypocenters moved well away from the initial 2.5 km depth imposed on the input data. A comparison of cluster locations is shown in Table 3 and Figure 3. The model selected to represent the results of the relocations is the Chelsea model. This model is consistent with all the others. Its cluster centroid while a little shallower than the other models is centrally located and retained the most earthquakes in the relocation process. The mean 2σ error is 164.7, 274.8, 362.4 meters for x (longitude), y (latitude), and z (depth) respectively. The final hypocenter relocations can be seen in Table 4 and Figure 4. As mentioned earlier the uncertainties provided by HypoDD provide good relative estimates. In order to address what the absolute uncertainties might be, we examined the maximum distance between all of the cluster centroids and the Chelsea model cluster centroid from Table 3. The greatest distances in cluster centroid from that of the Chelsea centroid are 160 m in longitude, 115 m in latitude, and 264 m in depth. Our absolute error could be considered the addition of the previous values to the relative locations uncertainties in Table 4. The total earthquake location uncertainties are shown in Figure 11b. A value for the Vp/Vs ratio of 1.73 was used in all of the relocations. Because the locations of these earthquakes rely on the high quality S-Wave phase arrivals this value can have a significant impact on the relocations of these events. An evaluation of the appropriate Vp/Vs ratio is well beyond the scope of this work and may be evaluated in the future. The uncertainties should be considered a minimum for the earthquake relocations given our assumption of the Vp/Vs ratio and the lack of nearby stations.

Table 3 – HypoDD relocation cluster centroids for the different velocity models used. The number of earthquakes that remained in the solution is shown in the last column. HypoDD eliminates earthquakes that occur above the surface or lose link to nearby earthquakes in the cluster.

Model	Latitude	Longitude	Depth (km)	Weighted RMS	Number of Earthquakes
Manitou	34.549496	-97.424278	2.764315	0.2263	37
Chelsea	34.550533	-97.424286	2.499614	0.21	43
Tryggvasson-Qualls	34.549976	-97.426025	2.695957	0.223	35
Central Oklahoma	34.551384	-97.423981	2.535471	0.2094	42

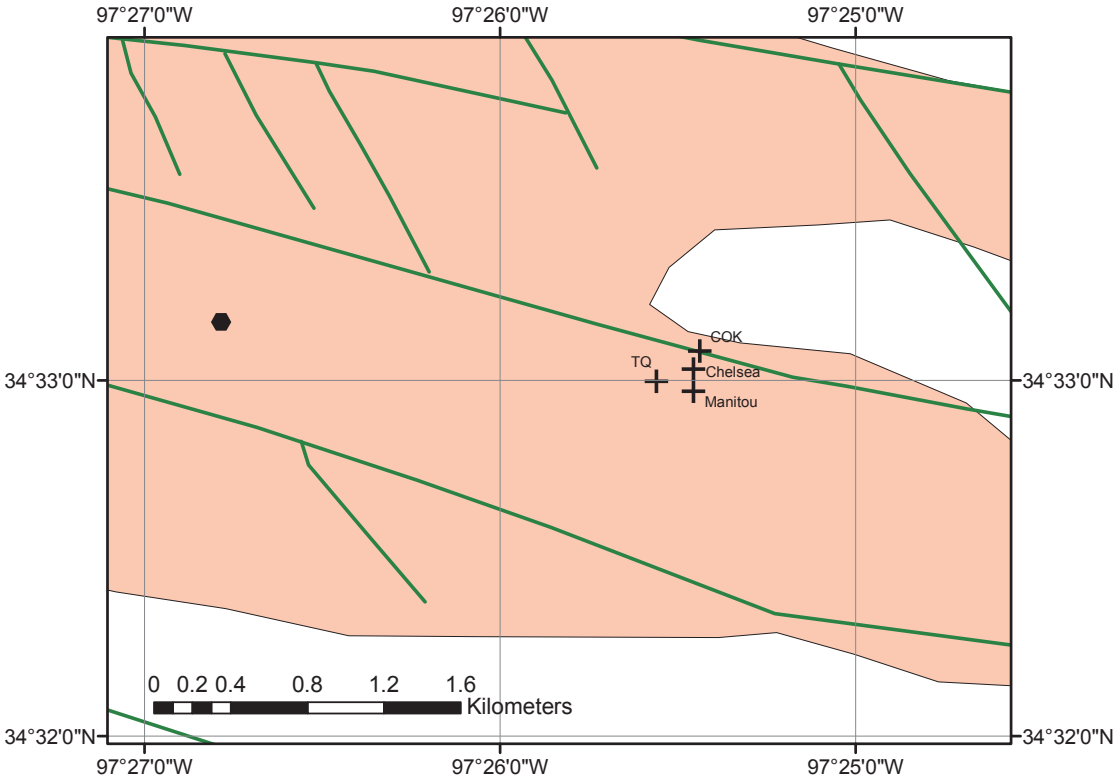

Figure 3 – HypoDD cluster centroid locations, black crosses, in relationship to Picket Unit B Well 4-18, shown as black hexagon, Eola Field (Boyd, 2002) is shown in salmon. Thick green lines are faults modified from Harlton (1964).

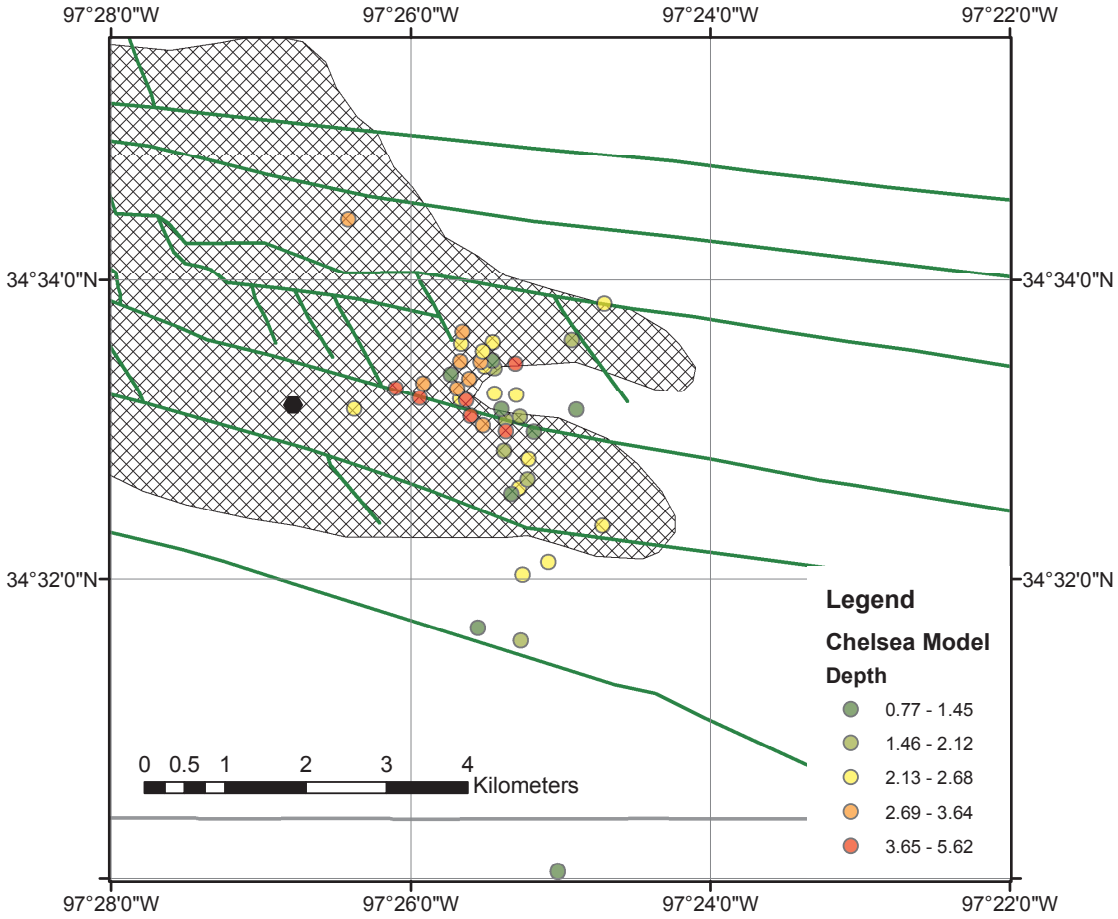

Figure 4 – HypoDD earthquake relocations (colored by depth in kilometers) determined using Chelsea model. Picket Unit B Well 4-18, shown as black hexagon, Eola Field (Boyd, 2002) shown cross-hachured area. Thick green lines are faults modified from Harlton (1964).

Table 4 – HypoDD relocations using the Chelsea velocity model. The mean 2σ error is 164.7, 274.8, 362.4 meters for longitude, latitude, depth respectively.

Latitude	Longitude	Depth (km)	Error Lon (m)	Error Lat (m)	Error Depth (m)	YR	MO	DY	HR	MN	SEC	Md
34.553837	-97.422	2.45	205.2	264.3	358.2	2011	1	17	19	35	37.44	1.9
34.559546	-97.428	2.39	235.3	391.8	532.4	2011	1	17	20	4	51.12	1.5
34.557353	-97.422	3.77	144.1	221.6	464.8	2011	1	17	20	16	7.02	2.1
34.556832	-97.424	1.84	148.8	240.8	772	2011	1	17	20	50	9	1.6
34.555636	-97.427	2.81	115.2	165.3	186.7	2011	1	17	20	56	49.06	2.1
34.557035	-97.425	2.25	200	269.5	383.9	2011	1	17	21	12	20.88	1.8
34.553377	-97.428	2.22	232.9	362.9	380.7	2011	1	17	21	23	32.24	1.7
34.533862	-97.421	2.6	170.8	410.1	339.1	2011	1	17	21	44	51.28	1.6
34.550916	-97.423	2.12	176	297.9	334.3	2011	1	17	21	46	37.08	2
34.543506	-97.421	2.68	220.3	570.2	423.3	2011	1	17	22	27	48.48	2.2
34.549756	-97.423	4.29	216.5	352.7	691	2011	1	17	22	35	5.12	2.3
34.573397	-97.44	3.64	388.1	506.7	1103	2011	1	17	23	37	1.44	1.6
34.544462	-97.42	1.69	131	206.4	233.1	2011	1	17	23	48	39.68	1.9
34.527926	-97.426	0.77	210.6	405.2	417.6	2011	1	17	23	52	24.38	1.4
34.553235	-97.427	3.98	159.3	286.9	590.6	2011	1	18	0	14	22.13	2.6
34.53527	-97.418	2.55	148.9	260.6	288.4	2011	1	18	0	33	39.44	1.7
34.539315	-97.412	2.36	220.7	352.5	450.5	2011	1	18	0	34	59.51	1.3
34.546712	-97.42	2.51	233.5	500.8	660.4	2011	1	18	0	46	46.76	1
34.557678	-97.424	1.45	152	236.7	300.8	2011	1	18	1	5	15.18	1.6
34.500814	-97.417	1.21	181	296.8	317	2011	1	18	1	6	31.9	1.2
34.55614	-97.429	1.29	135.3	183	215.4	2011	1	18	1	31	43.79	1.7
34.555119	-97.432	2.83	145.8	270.8	275	2011	1	18	1	37	0.57	1.7
34.554578	-97.435	4.63	164.9	231.3	445.2	2011	1	18	1	40	42.24	2.2
34.560836	-97.428	3.11	112.8	160.9	232.3	2011	1	18	2	13	20.17	2
34.559957	-97.415	1.61	141.1	243.4	306.8	2011	1	18	2	27	32.86	1.5
34.557605	-97.428	3.21	162.9	253.9	409.5	2011	1	18	2	43	34.24	2
34.55968	-97.424	2.21	183.7	235.2	287.1	2011	1	18	3	17	27.51	1.8
34.554517	-97.428	3.08	115.2	182.8	284.4	2011	1	18	3	40	6.62	2.8
34.54281	-97.422	1.4	102.6	185.6	177.7	2011	1	18	4	1	53.34	2.4
34.563953	-97.412	2.37	169	275.2	321.8	2011	1	18	4	53	0.09	1.5
34.552193	-97.423	1.24	131.9	238.8	273.3	2011	1	18	5	57	58.97	2.1
34.552287	-97.44	2.31	98.6	166.7	190.5	2011	1	18	7	5	49.79	1.2
34.552144	-97.415	1.12	157.5	218	300.5	2011	1	18	7	58	42.51	1.2
34.55752	-97.426	2.97	133.8	301.8	259.9	2011	1	18	7	59	50.63	1.3
34.553984	-97.424	2.47	125.8	247.6	215.7	2011	1	18	8	23	5.25	1.7
34.553451	-97.432	3.81	126.5	265.4	296.6	2011	1	18	9	22	43.89	2.3
34.547607	-97.423	1.93	133.6	240.6	241.5	2011	1	18	9	52	43.55	1.5
34.558683	-97.425	2.58	107.2	164	160.9	2011	1	18	12	32	53.83	2
34.526497	-97.421	1.9	182	271.3	305.6	2011	1	18	12	43	57.78	1.5
34.550395	-97.425	3.02	148.8	251.6	248.9	2011	1	18	19	40	5.34	1.4
34.55144	-97.427	5.62	200.3	245.5	401.5	2011	1	19	4	29	55.61	2
34.551355	-97.421	2.09	107.2	188.9	214.1	2011	1	22	13	8	10.84	2.1
34.549731	-97.42	1.12	106.6	195.2	292.5	2011	1	22	15	6	49.46	2

Summary of Earthquake Activity

The earthquake activity in southern Garvin County began at 1/17/11 19:19 UTC and there were 43 earthquakes large enough to be located by 1/19/11 4:29 UTC. Of these events, 39 earthquakes occurred by 1/18/11 9:52 UTC, with largest having a duration magnitude of 2.8 (Md) and the smallest a Md 1.0. The timing of these events can be seen in Figures 5 and 6. The first earthquake began about 1 hour and 20 minutes after hydraulic-fracturing operations had ceased.

The earthquakes exhibited waveforms with an unusual character. A comparison of waveform recordings between one of the larger earthquakes in the southern Garvin County earthquake sequence, that occurrued on January 18th, and an earthquake that occurred a little bit further north in Garvin county, on January 25th, of the same magnitude are shown in Figures 7, 8 and 9. The unique character of these events which make them appear different than other regionally recorded earthquakes are:

- The events are clearly shallow and generate significant surface wave energy
- P-waves are:
  - Subdued in amplitude
  - Not impulsive even on the closest stations
  - Significant energy in the P-coda (ringing)
  - Nearly as prominent on horizontal as vertical components
  - Very hard to identify on all but the nearest seismic stations
  - Could not be identified using cross correlation, generally correlating better to an arrival sometime after the S-wave
- S-waves are:
  - Somewhat difficult to distinguish from P-coda and because of the significant surface wave energy
  - Easiest phase to identify on most seismic stations
  - Identifiable using cross correlation as well

These characteristics definitely suggest that the shallow hypocenter locations are most likely not an artifact of the location algorithm (program) or velocity model. Any other conclusions about the unique character of these events would be speculative.

The earthquakes occur within the portion of the Eola field, which has many small fault bounded blocks. The seismicity appears consistent with activation on portions of these fault bounding blocks or smaller faults within the blocks. Due to the character of the P-wave arrivals it was not possible to produce first motion focal mechanisms for these earthquakes. The majority of the earthquakes occur within 4 km horizontal distance from the Picket Unit B well.

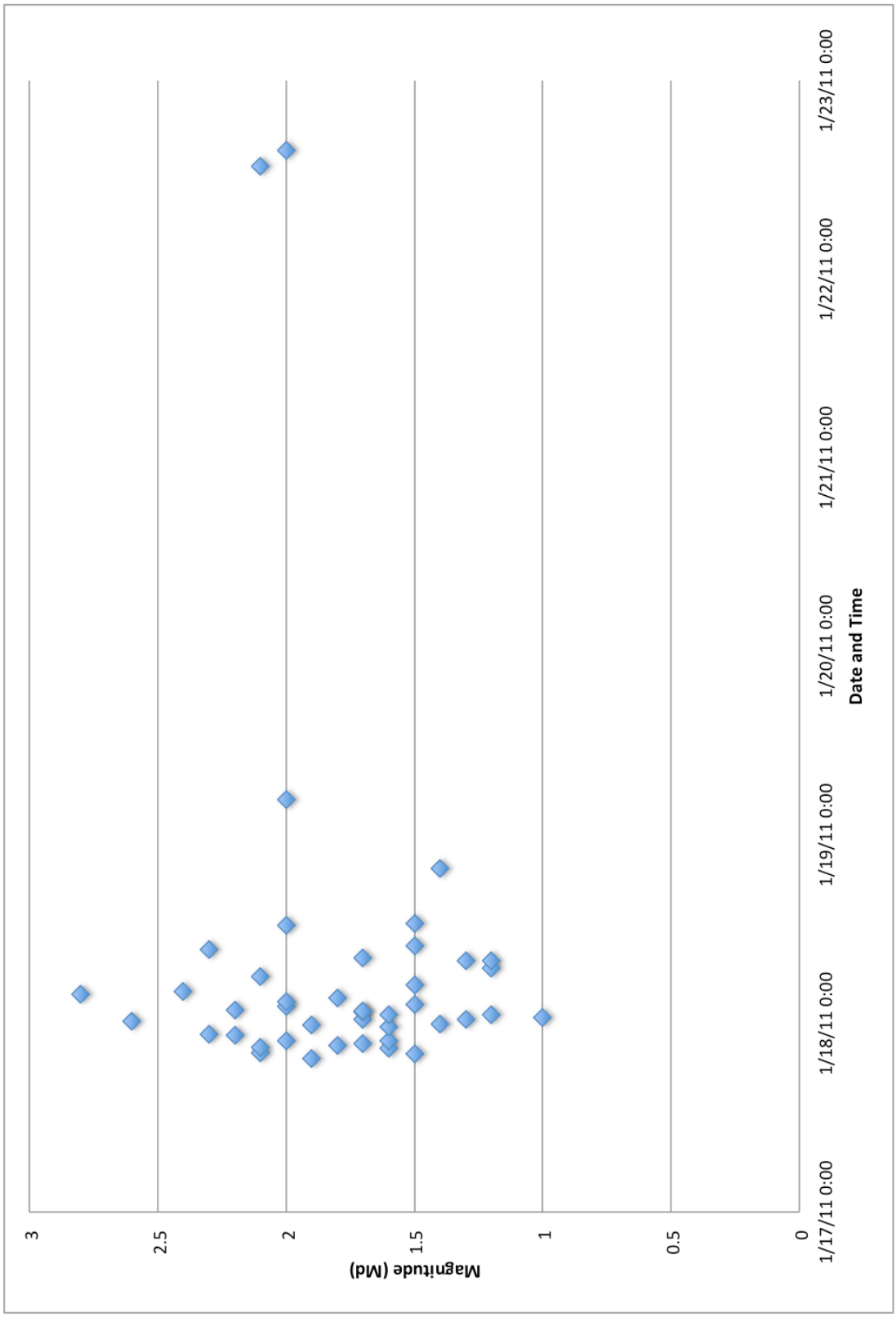

Figure 5 – Time magnitude plot of Eola Field earthquakes following hydraulic fracturing at Picket Unit B Well 4-18. Hydraulic fracturing began at about 1/17/11 12:00.

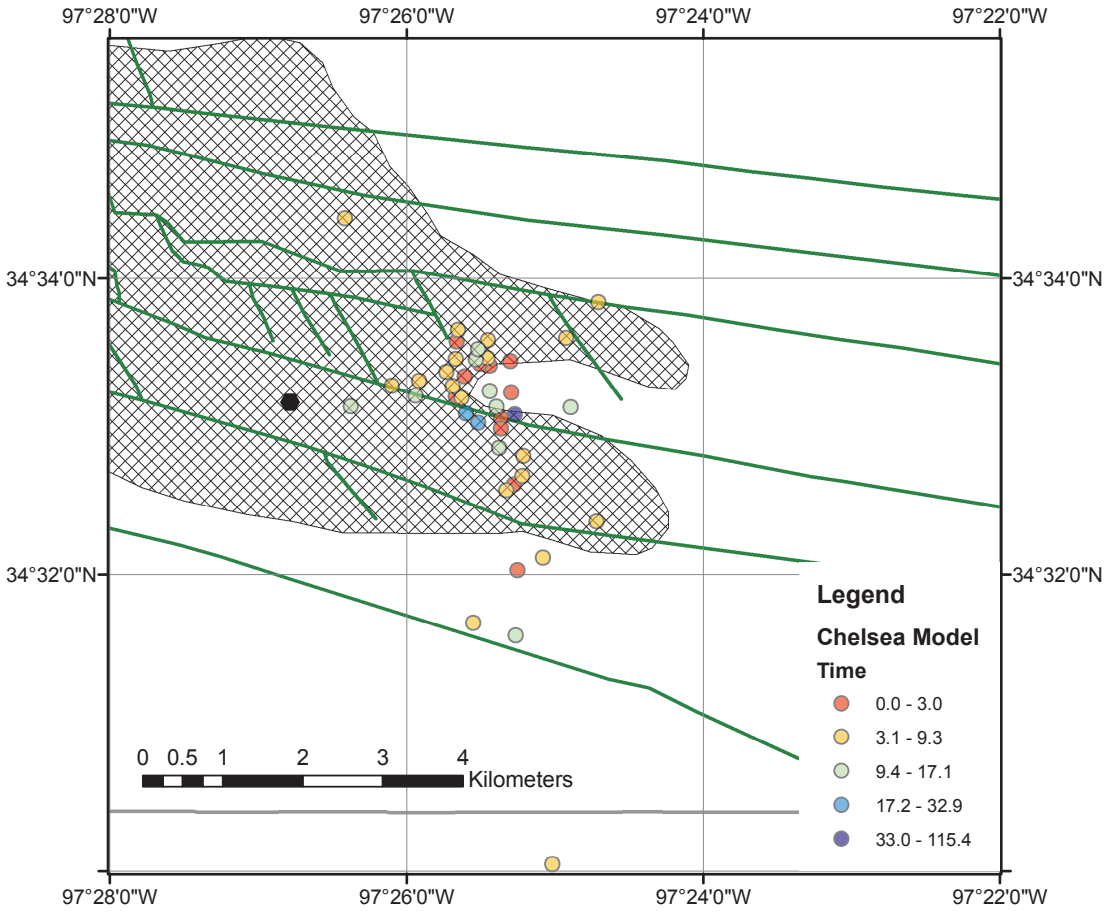

Figure 6 – HypoDD relocations using the Chelsea velocity model; symbols are colored by the number of hours after the first earthquake observed in the Eola Field. Picket Unit B Well 4-18, shown as black hexagon, Eola Field (Boyd, 2002) shown cross-hachured area. Thick green lines are faults modified from Harlton (1964).

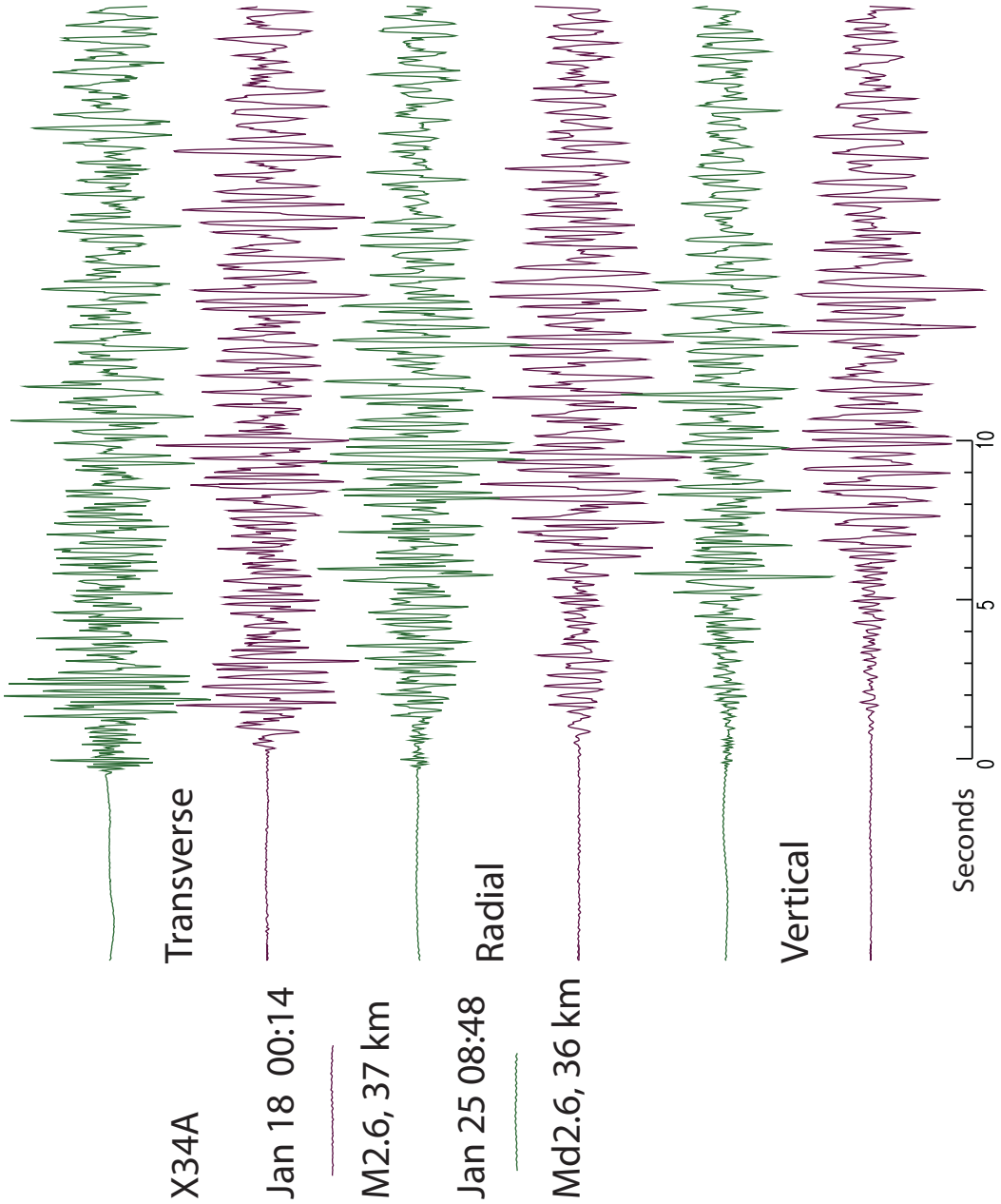

Figure 7 – Comparison of two similar sized earthequakes recorded at station X34A in Garvin County. The earthquake on Jan. 18 occurred in the Enola Field and the earthquake on Jan 25 occurred further to the north at about the same epicentral distance. The waveforms are aligned on each events corresponding origin time.

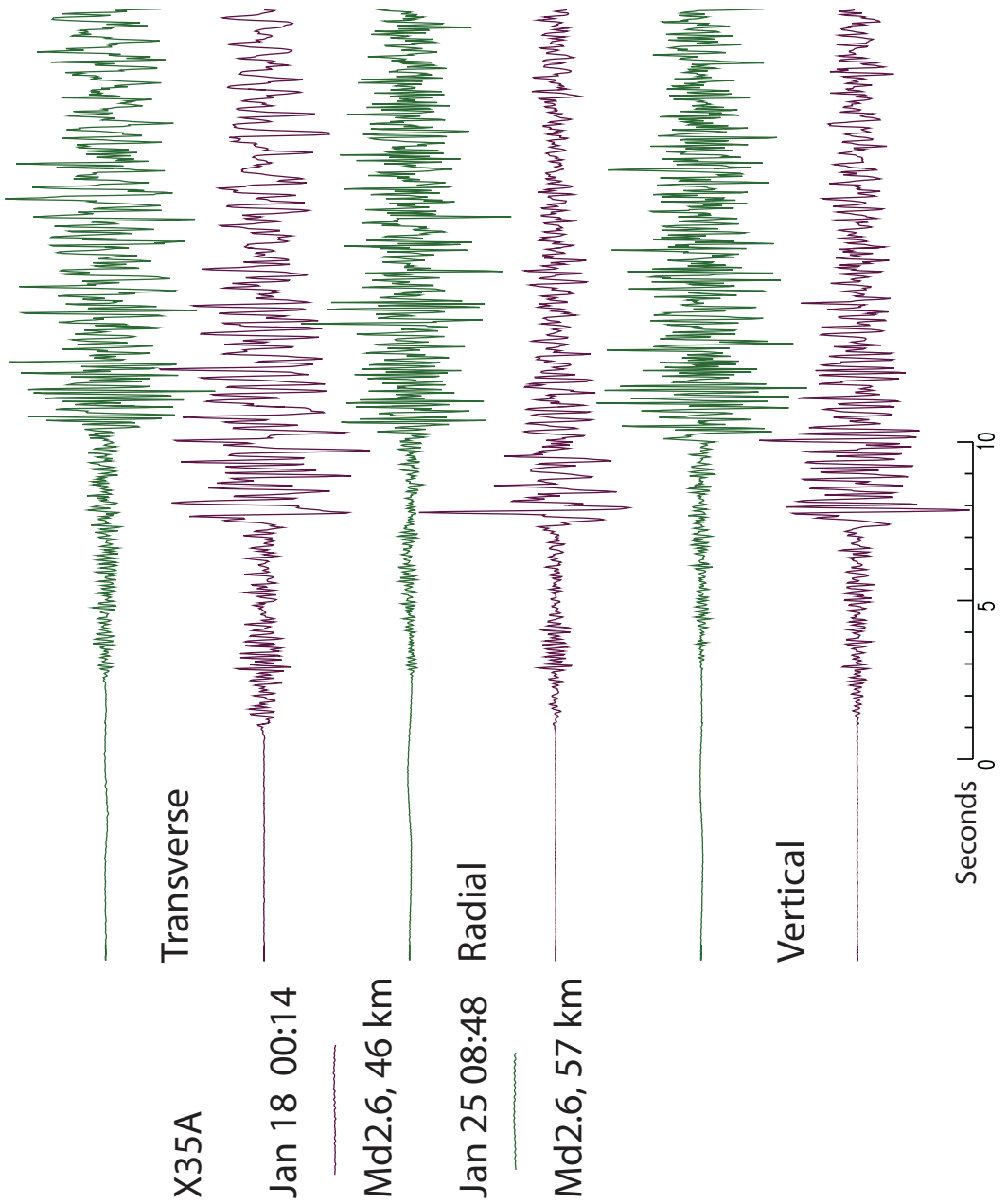

Figure 8 – Comparison of two similar sized earthequakes recorded at station X34A in Garvin County. The earthquake on Jan. 18 occurred in the Enola Field and the earthquake on Jan 25 occurred further to the north. The waveforms are aligned on each events corresponding origin time.

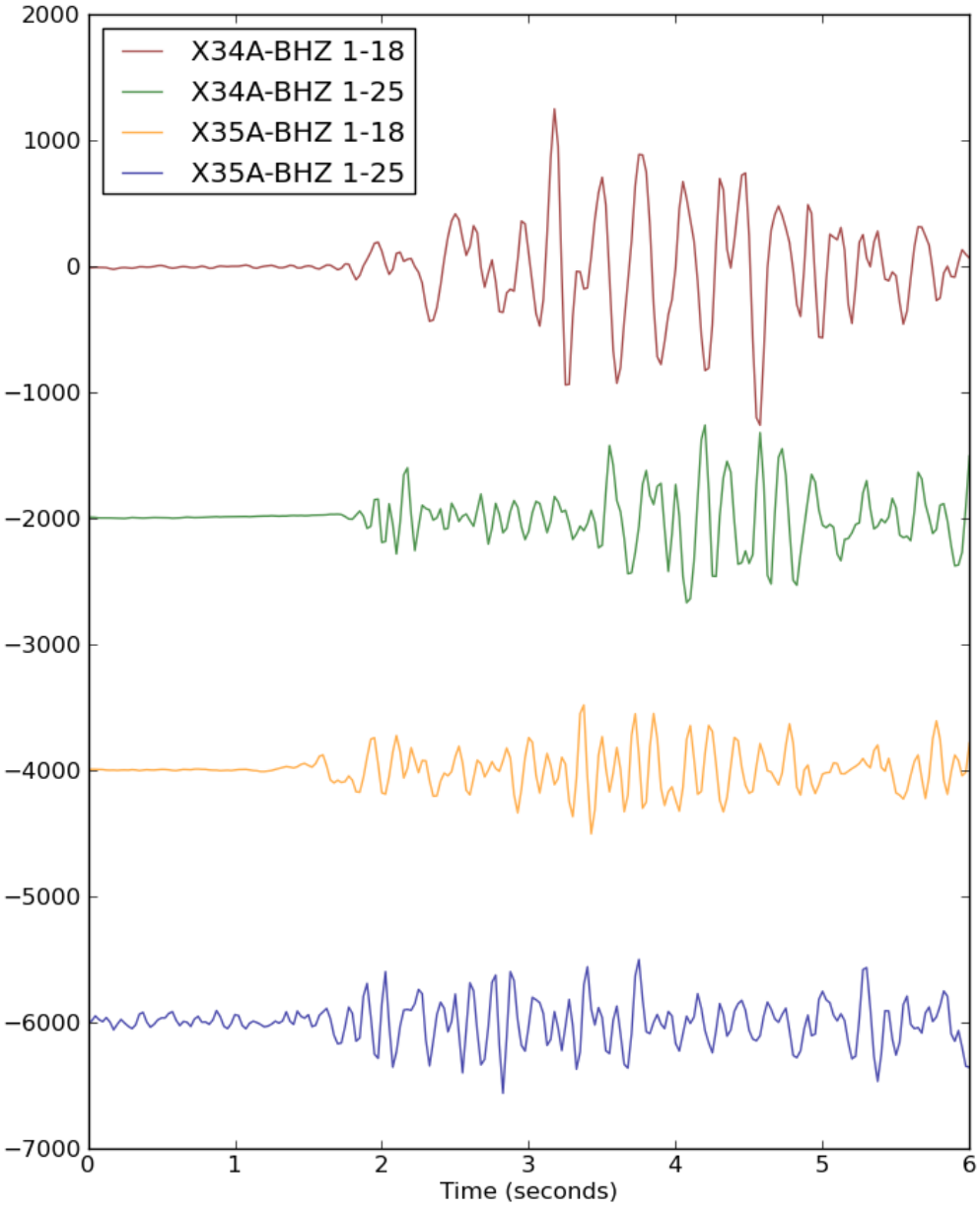

Figure 9 – Comparison of P-Wave arrivals for the two events compared in Figures 7 and 8. P-waves for the Jan. 18th Eola Field earthquake have lower frequency arrivals than those from the earthquake on Jan. 25th.

Discussion

Anthropogenic triggered seismicity has regained scientific and media attention recently. Recent earthquakes in the Dallas-Fort Worth area (Frohlich et al., 2011) and earthquakes near Guy, Arkansas, have dramatically raised this issue to some significance. Cases of clear anthropogenically-triggered seismicity from fluid injection are well documented with correlations between the number of earthquakes in an area and injection, specifically injection pressures, with earthquakes occurring very close to the well. Examples of clearly induced seismicity include the Rocky Mountain Arsenal (Hsieh and Bredehoeft, 1981), Rangely, Colorado (Raleigh et al., 1972; Raleigh et al., 1976), Paradox Valley, Colorado (Ake et al., 2005), and the KTB Deep Well in Germany (Jost et al., 1995; Baisch et al., 2002). There are also many examples from enhanced geothermal systems where there is a clear correlation between injection and earthquakes. Examples of these include, but are not limited to Frenton Hill, New Mexico (Fehler et al., 1998), Basel, Switzerland (Deichmann and Giardini, 2009), Cooper Basin, Australia (Baisch et al., 2006), and Soultz, France (Horalek et al., 2010). Figure 10 demonstrates the earthquake distribution as a function of distance from the well for a few of these cases. In the cases from Rangely, Colorado and the Rocky Mountain Arsenal the majority of seismicity lies within a distance of 4 km from the injection well, which is quite comparable to what is seen for the Picket Unit B well in this study.

There are also less clear examples in which earthquakes may or may not have been triggered by fluid injection at a well. In these cases, there is no clear correlation between fluid injection and earthquakes and the earthquakes may occur at somewhat larger distances from the suspected wells. Some examples of these cases are Sleepy Hollow Oil Field, Nebraska (Rothe and Lui, 1983; Evans and Steeples, 1987); a gas field, Lacq France (Grasso and Wittlinger, 1990); a deep waste disposal well in northeastern Ohio (Nicholson et al., 1988; Seeber et al., 2004); Fashing, Texas (Davis et al., 1995); the Wabash Valley, Illinois (Eager et al., 2006), and the DFW airport (Frohlich et al., 2011). These are not exhaustive lists of proposed induced seismicity and there is a large spectrum of scientific opinions regarding many of these cases.

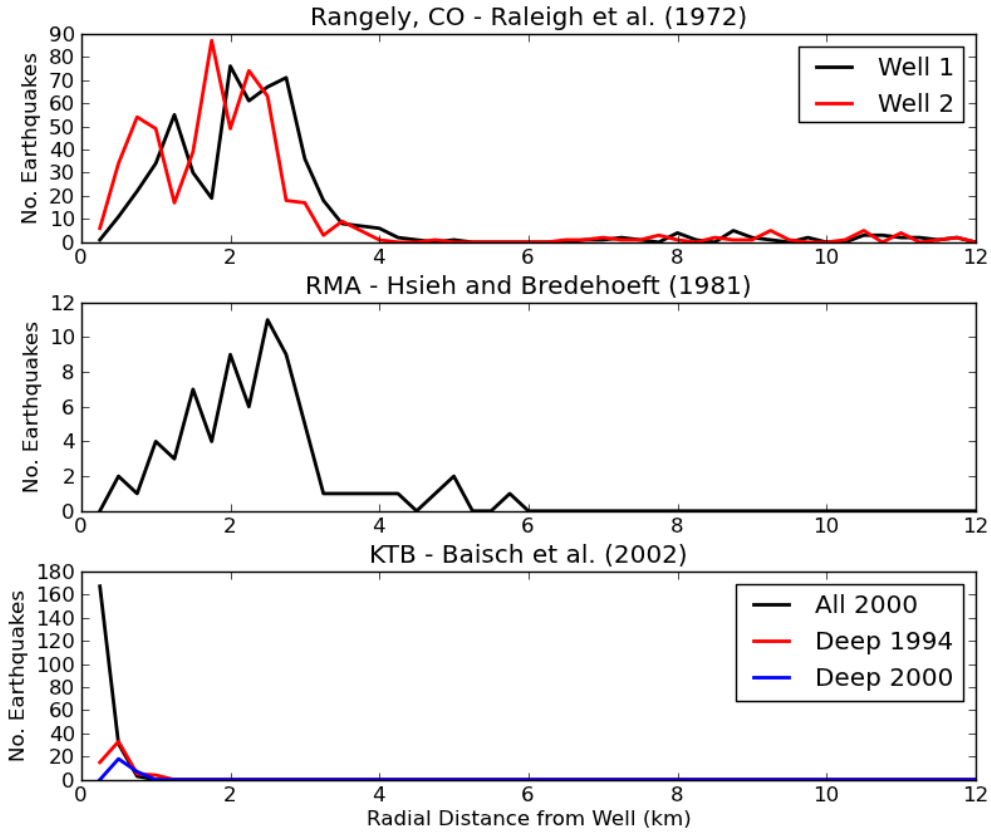

Figure 10 – Number of earthquakes verses distance for selected examples where seismicity is clearly induced from fluid injection at depth. The information was hand digitized from Raleigh et al. (1972), Hsieh and Bredehoeft (1981), and Baisch et al. (2002). The bin size used is 0.25 km.

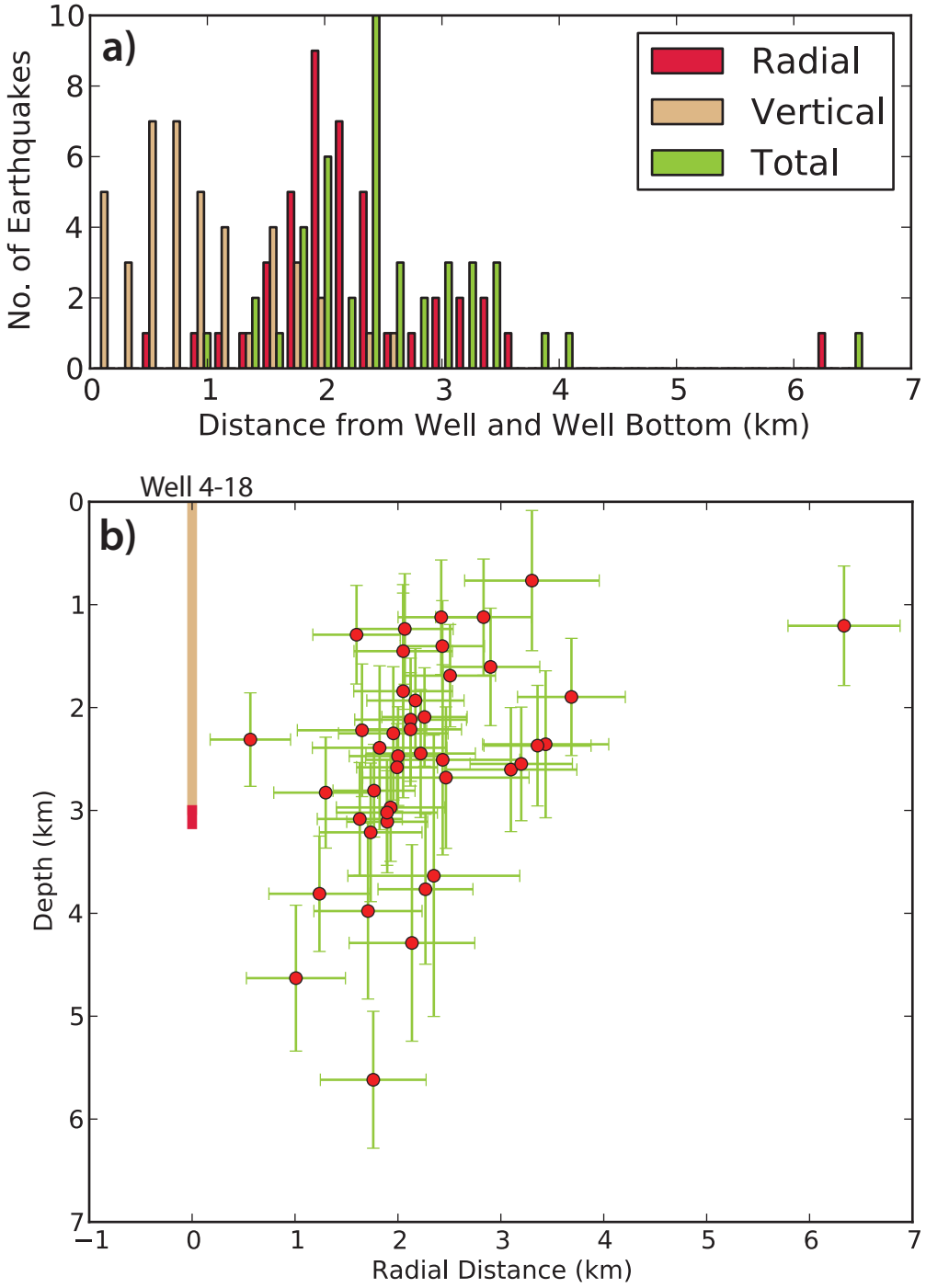

Figure 11 – a) Number of earthquakes plotted versus distance from the Picket Unit B Well 4-18. Total and vertical distances were determined relative to the central depth of hydraulic fracturing stage 1. b) Spatial distribution of earthquakes in relationship to Well 4-18 with estimated absolute location error shown as green crosses. The depth interval for the first frac stage is shown as the crimson portion of the well.

Davis and Frolich (1993) outlined seven questions to help aid in examining whether or not earthquakes may have been induced by fluid injection at depth. We will examine these seven questions in relation to the hydraulic fracturing of the Picket Unit B and the earthquakes observed in the Eola Field in Garvin County. Affirmative answers to all seven questions according to Frolich and Davis (1993) would indicate that earthquakes are clearly induced.

Question 1: Are these events the first known earthquakes of this character in the region? (UNKOWN)
Given the analog recording history for most of the Oklahoma Geological Survey's recording history it is difficult to determine whether the character is uniquely different from that of earthquakes previously observed in the area. There have been significant numbers of earthquakes occurring in this area in the past, Figure 1. This negative response by itself would suggest that hydro-fracturing at Picket Unit B did not induce these earthquakes. However, we will examine all of the criteria outlined by Davis and Frolich (1993).

Question 2: Is there a clear correlation between injection and seismicity? (YES)
There is a clear correlation between the time of hydraulic-fracturing and the observed seismicity in the Eola Field. However, subsequent hydraulic-fracturing stages at Picket Unit B Well 4-18 did not appear to have any earthquakes associated with them. Subsequent frac stages were all shallower than the first, and otherwise there were no major differences in the fracking operations.

Question 3: Are epicenters near wells (within 5 km)? (YES)
Nearly all earthquakes are located within this distance and the majority of earthquakes are closer than the 5 km specified by Davis and Frolich (1993). The 5 km was selected somewhat arbitrarily by Davis and Frolich (1993) and may not be completely appropriate. The earthquakes hypocenters have formal uncertainties from HypoDD, including our uncertainty in velocity model, of about 320 m in longitude and 490 m in latitude. These uncertainties represent the absolute minimum of what we should consider the location error to be. Unknown effects of different Vp/Vs ratios and other factors add to the actual error in location being larger. Figure 11 demonstrates the distance of earthquakes from the well.

Question 4: Do some earthquakes occur at or near injection depths? (YES)
Most of the earthquakes do occur near injection depths. The minimum uncertainty in focal mechanism depths should be considered approximately 630 m. The focal depth is the least well-constrained portion of the hypocenter location and reported depths should be considered somewhat suspect since there are no stations within a few kilometers of the earthquake sequence. The waveform characteristics are consistent with the shallow focal depths from the double-differencing relocation. hypocentral depths and formal uncertainties can be seen in Figure 11b.

Question 5: If not, are there known geologic structures, that may channel flow to sites of earthquakes? (YES)
There are significant structures within the Eola Field. The near vertical block bounding faults provide a pathway for fluid flow in the subsurface. In addition faults are rarely single entities but rather a complex network of faults and fractures increasing the number of structures that could potentially channel flow (Scholz, 1990). The average error in depth should be considered to be at a minimum 630 m and should be expected to be larger since there are no nearby stations to help constrain the focal depth.

Question 6: Are changes in fluid pressure at well bottoms sufficient to encourage seismicity? (YES)
Clearly since the case considered here involves hydraulic-fracturing where pressure is being used to fracture rock, by design the pressures are sufficient to encourage seismicity.

Question 7: Are changes in fluid pressure at hypocentral locations sufficient to encourage seismicity? (UNKNOWN)
A further examination of this question is provided below. It is possible to apply a reasonable physical model that suggests the hydraulic fracturing could have increased pressures at hypocentral locations. With all the production that has occurred within the Eola Field and our uncertainty in subsurface structure it would be difficult if not impossible to accurately model the effects of a pressure pulse at hypocentral locations. This is especially true given the uncertainties in earthquake locations in this study.

After having evaluated the above criteria we have five affirmative responses and two uncertain responses. Is this enough to determine that these earthquakes were triggered or not? At this point I would like to directly quote Davis and Frolich (1993).

> *"At present it is impossible to predict the effects of injection with absolute certainty. This uncertainty arises both because the underlying physical mechanisms of earthquakes are poorly understood, and because in nearly every specific situation there is inadequate or incomplete information about regional stresses, fluid migration, historical seismicity, etc. Clearly, a series of seven or ten yes or no questions oversimplifies many of these issues."*

This statement reflects the incredible complexity and uncertainty for most cases in associating anthropogenic causes and earthquakes.

The physical mechanism, which could trigger these earthquakes from the hydraulic fracturing operations at the Picket Unit B well, is the diffusion of pore-pressure interacting with a pre-existing structure to initiate earthquakes on a fault or fracture that has an orientation favorable to failure within the regional stress field. Many researchers have described the migration of induced seismicity by describing the migration of a pressure front through the diffusion of pore pressure, hydraulic

diffusivity (Talwani and Acree, 1985; Nicholson and Wesson, 1990; Shapiro et al., 1999; Rothert and Shapiro, 2003; Rozhko, 2010). Cornet (2000) argued that the shape of microseismicity is controlled by the fracture process and hydromechanical coupling rather than a homogeneous hydraulic diffusivity through a rock mass. Rutledge et al. (2004) describe this behavior in detail for a closely monitored hydraulic fracturing within the Carthage Cotton Valley Gas Field, Texas. They clearly demonstrate the control of the regional stress field, pressure diffusion, interaction with existing structures and suggest that there is a significant amount of aseismic slip occurring within the fractured volume.

In order to examine whether or not the data for this earthquake sequence would fit a pore pressure diffusion model we used the simplified pore pressure diffusion model of Talwani and Acree (1985). This method describes the pore pressure diffusion through time through via a diffusion constant called seismic hydraulic diffusivity. This hydraulic diffusivity can be related to the physical properties of the rocks and fluids involved such as fluid viscosity, rock porosity and permeability, and the compressibility of the fluid and rocks. There is a simple method to determine the seismic hydraulic diffusivity (α),

$$\alpha = \frac{L^2}{t}$$

where L is the distance of the earthquake away from the well in centimeters (cm) and t is the time, in seconds, since injection began. Talwani and Acree (1985) found that seismic hydraulic diffusivity for the cases they examined ranged from $5x10^3$ to $6x10^5$ cm^2/s. For our case we determined the seismic hydraulic diffusivity which fit 95% of the earthquakes was $2.8x10^6$ to $2.6x10^6 cm^2/s$ depending on whether this was determined for the total hypocentral distance from the center point of the injection interval or simply the radial distance from the well. The hydraulic diffusivity can be related to permeability from the following relationship.

$$\alpha = \frac{k}{\mu \phi \beta_F}$$

where,

k – is the permeability

μ – is the viscosity of water (10^{-8} bar/s)

ϕ – is the porosity of fractured rock ($3x10^{-3}$ for this example, and

β_F = is the effective compressibility of the fluid ($3x10^{-5}$ bar^{-1}).

This provides a maximum permeability needed to describe this earthquake sequence of 255 milliDarcies (mD). In this example the uncertainties in earthquake locations are not considered (Figure 12). While this permeability may seem high for a shale it is within the values reported for in situ rocks, especially fractured rock (Brace, 1984).

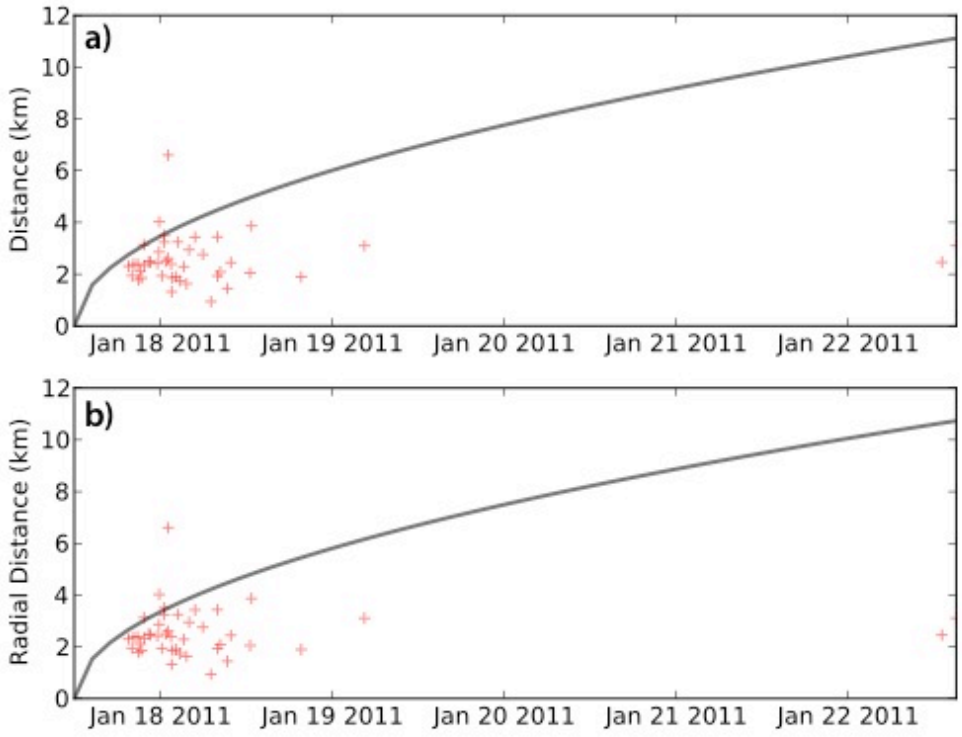

Figure 12 – a) Pore pressure diffusion model results shown for total distance from Picket Unit B Well 4-18. Red crosses show earthquake locations relative to the midpoint of the first hydraulic fracturing stage, and the solid black line represents location at a specific time of the pore pressure front from the model. Earthquakes plotted above this line are inconsistent with this pore pressure diffusion model, and all earthquakes plotted below this line are consistent with this pore pressure diffusion model. This line represents a seismic hydraulic diffusivity of 2.8×10^6 cm^2/s, which is roughly equivalent to a permeability of 255 milliDarcies (mD), and represents the distance from the well of a pressure front. b) Same as for (a) except only the radial distance is considered. The resultant seismic hydraulic diffusivity is $2.6 \times 10^6 cm^2/s$.

Conclusions

Determining whether or not earthquakes have been induced in most portions of the stable continent is problematic, because of our poor knowledge of historical earthquakes, earthquake processes and the long recurrence intervals for earthquakes in the stable continent. In addition understanding fluid flow and pressure diffusion in the unique geology and structures of an area poses real and significant challenges. The strong spatial and temporal correlations to the hydraulic-fracturing in Picket Unit B Well 4-18 certainly suggest that the earthquakes observed in the Eola Field could have possibly been triggered by this activity. Simply because the earthquakes fit a simple pore pressure diffusion model does not indicate that this is the physical process that caused these earthquakes. The number of historical earthquakes in the area and uncertainties in hypocenter locations make it impossible to determine with a high degree of certainty whether or not hydraulic-fracturing induced these earthquakes.

Whether or not the earthquakes in the Eola Field were triggered by hydraulic-fracturing these were small earthquakes with only one local resident having reported feeling them. While the societal impact of understanding whether or not small earthquakes may have been caused by hydraulic-fracturing may be small, it could potentially help us learn more about subsurface properties such as stresses at depth, strength of faults, fluid flow, pressure diffusion, and long term fault and earthquake behaviors of the stable continent. It may also be possible to identify what criteria may affect the likelihood of anthropogenically induced earthquakes and provide oil and gas operators the ability to minimize any adverse affects as suggested by Shapiro et al. (2007).

Acknowledgements

The NSF Earthscope Project and the Transportable Array stations and data availability provided by IRIS made this work possible. I would also like to thank Amie Gibson, Dr. Kenneth V. Luza, and Dr. G. Randal Keller for their helpful comments and suggestions for this paper. Russell Standbridge, OGS Cartography, provided a great deal of technical advice and information. I would also like to thank the Oklahoma Corporation Commission for the help in obtaining information and input to this effort. I would also like to thank Cimarex Energy Co. for providing usefull technical information about the hydraulic fracturing of Picket Unit B Well 4-18.

References

Ake, J., K. Mahrer, D. O'Connell, and L. Block, 2005, Deep-Injection and Closely Monitored Induced Seismicity at Paradox Valley, Colorado, *Bull. Seismol. Soc. Amer.*, **95(2)**, p. 664-683.

Baisch, S., M. Bohnhoff, L. Ceranna, Y. Tu, and H.P. Harjes, 2002, Probing the Crust to 9-km Depth: Fluid-Injection Experiments and Induced Seismicity at the KTB Superdeep Deep Drilling Hole, Germany, *Bull. Seismol. Soc. Amer.*, **92(6)**, p. 2369-2380.

Baisch, S., R. Weidler, R. Voros, D. Wyborn, and L. de Graaf, 2006, Induced Seismicity during the Stimulation of a Geothermal HFR Resevior in the Cooper Basin, Australia, *Bull. Seismol. Soc. Amer.*, **96(6)**, p. 2242-2256.

Boyd, D.T., 2002, Map of Oklahoma Oil and Gas Fields, Okahoma Geologicial Survey **GM36**.

Brace, W.F., 1984, Permeability of Crystalline Rocks: New In Situ Measurements, *J. Geophys. Res.*, **89(B6)**, p. 4327-4330.

Davis, S.D. and C. Frohlich, 1993, Did (or Will) Fluid Injection Cause Earthquakes? – Criteria for a Rational Assessment, *Seismol. Res. Lett.*, **64(3-4)**, p. 207-224.

Davis, S.D., P.A. Nyffenegger, and C. Frohlich, 1995, The 9 April 1993 Earthquake in South-Central Texas: Was It Induced by Fluid Withdrawal?, *Bull. Seismol. Soc. Amer.*, **85(6)**, p. 1888-1895.

Eager, K.C., G.L. Pavlis, and M.W. Hamburger, 2006, Evidence of Possible Induced Seismicity in the Wabash Valley Seismic Zone from Improved Microearthquake Locations, *Bull. Seismol. Soc. Amer.*, **96(5)**, p. 1718-1728.

Evans, D.G. and D.W. Steeples, 1987, Microearthquakes near the Sleepy Hollow Oil Field, Southwestern Nebraska, *Bull. Seismol. Soc. Amer.*, **77(1)**, p. 132-140.

Fehler, M., L. House, W.S. Phillips, and R. Potter, 1998, A method to allow temporal variation of velocity in travel-time tomography using microearthquakes induced during hydraulic fracturing, *Tectonophysics*, **289**, p. 189-201.

Frohlich, C., C. Hayward, B. Stump, and E. Potter, 2011, The Dallas-Fort Worth Earthquake Sequence: October 2008 through May 2009, *Bull. Seismol. Soc. Amer.*, **101(1)**, p. 327-340.

Deichmann, N. and D. Giardini, 2009, Earthquakes Induced by the Stimulation of an Enhanced Geothermal System below Basel, Switzerland, *Seismol. Res. Lett.*, **80(5)**, p. 784-798.

Granath, J.W., 1989, Structural Evolution of the Ardmore Basin, Oklahoma: Progressive Deformation in the Foreland of the Ouichita Collision, *Tectonics*, **8(5)**, p. 1015-1036.

Grasso, J. R. and G. Wittlinger (1990). Ten Years of Seismic Monitoring Over a Gas Field, Bull. Seismol. Soc. Amer. **80**(2): 450-473.

Harlton, B.H., 1964, Tectonic Framework of Eola and Southeast Hoover Oil Fields and West Timbered Hills Area, Garvin and Murray Counties, Oklahoma, *Bull. Amer. Assoc. Petrol. Geol.*, **48(9),** p 1555-1567.

Havskov, J. and L. Ottemoller, 1999, SeisAn Earthquake Analysis Software, *Seis. Res. Lett.*, **70**.

Horalek, J., Z. Jechumtalova, L. Dorbath, and J. Sileny, 2010, Source mechanisms of micro-earthquakes induced in a fluid injection experiment at the HDR site Soultz-sous-Forets (Alsace) in 2003 and their temporal and spatial variations, *Geophys. J. Int.*, **181**, p. 1547-1565.

Hsieh, P.A. and J.D. Bredehoeft, 1981, A Resevoir Analysis of the Denver Earthquakes: A Case of Induced Seismicity, *J. Geophys. Res.*, **86(B2),** p. 903-920.

Jost, M.L., T. BuBelberg, O. Jost, H.P. Harjes,1995, Source Parameters of Injection-Induced Microearthquakes at 9 km Depth at the KTB Deep Drilling Site, Germany, *Bull. Seismol. Soc. Amer.*, **88(3)**, p. 815-822.

Keller, G.R., E.G. Lidiak, W.J. Hinze, and L.W. Braile, 1983, The Role of Rifting in the Tectonic Development of the Midcontinent, U.S.A., *Tectonophysics*, **94**, p. 391-412.

Lawson, J.E. Jr. and K.V. Luza, 2006, Oklahoma Earthquakes 2005, *Oklahoma Geology Notes*, **V. 66, No. 3**, Fall 2006.

Lienert, B. R. E., E. Berg, and L.N. Frazer, 1986, Hypocenter: An earthquake location method using centered, scaled, and adaptively least squares, *Bull. Seismol. Soc. Am.*, **76**, p. 771–783.

Lienert, B. R. E. and J. Havskov, 1995, A computer program for locating earthquakes both locally and globally, *Seismol. Res. Lett.*, **66**, p. 26–36.

McCaskill, J.G. Jr., 1998, Multiple Stratigraphic Indicators of Major Strike-Slip Movement Along the Eola Fault, Subsurface, Arbuckle Mountains, Oklahoma, Shale Shaker, p. 119-133.

Mitchell, B.J. and M. Landisman, 1970, Interpretation of a Crustal Section across Oklahoma, *Geol. Soc. Amer. Bul.*, **81(9)**, p. 2647-2656.

Nicholson, C., E. Roeloffs, and R.L. Wesson, 1988, The Northeastern Ohio Earthquake of 31 January 1986: Was It Induced?, *Bull. Seismol. Soc. Amer.*, **78(1)**, p. 188-217.

Nicholson, C. and R.L. Wesson, 1990, Earthquake Hazard Associated With Deep Well Injection – A Report to the U.S. Environmental Protection Agency, U.S. Geol. Surv. Bull, **1951**, pp. 74.

Northcutt, R.A. and J.A., Campbell, 1995, Geologic provinces of Oklahoma, *Oklahoma Geological Survey* **OF5-95**.

Raleigh, C.B., J.H. Healy, and J.D. Bredehoeft, 1972, Faulting and Crustal Stress at Rangely, Colorado, *Am. Geophys. Union Geophys. Monograph*, **16**, p. 275-284.

Raleigh, C.B., J.H. Healy, and J.D. Bredehoeft, 1976, An Experiment in Earthquake Control at Rangely, Colorado, *Science*, **191**, p. 1230-1237.

Rothe, G.H. and C.Y. Lui, 1983, Possibility of Induced Seismicity in the Vicinity of the Sleepy Hollow Oil Field, Southwestern Nebraska, *Bull. Seismol. Soc. Amer.*, **73(5)**, p. 1357-1367.

Rothert, E. and S.A. Shapiro, 2003, Microseismic monitoring of borehole fluid injections: Data modeling and inversion for hydraulic properties of rocks, *Geophysics*, **68(2)**, p. 685-689.

Rozhko, A.Y., 2010, Role of seepage forces on seismicity triggering, *J. Geophys. Res.*, **115**, doi:10.1029/2009JB007182.

Rutledge, J.T., W.S. Phillips, and M.J. Mayerhofer, 2004, Faulting Induced bye Forced Fluid Injection and Fluid Flow Forced by Faulting: An Interpretation of Hydraulic-Fracture Microseismicity, Carthage Cotton Valley Gas Field, Texas, *Bull Seismol. Soc. Amer.*, **94(5)**, p. 1817-1830.

Scholz, C.H., 1990, The Mechanics of Earthquakes and Faulting, *Cambridge University Press,* pp. 439.

Seeber, L., J.G. Armbruster, and W.Y. Kim, 2004, A Fluid-Injection Earthquake Sequence in Ashtabula, Ohio: Implications for Seismogenesis in Stable Continental Regions, *Bull. Seismol. Soc. Amer.*, **94(1)**, p. 76-87.

Shapiro, S.A., P. Audigane, and J.J. Royer, 1999, Large-scale in situ permeability tensor of rocks from induced microseismicity, *Geophys. J. Int.*, **137**, p. 207-213.

Shapiro, S.A., C. Dinske, and J. Kummerow, 2007, Probability of a given-magnitude earthquake induced by a fluid injection, *Geophys. Res. Lett.*, **34**.

Stoeser, D.B., G.N. Green, L.C. Morath, W.D. Heran, A.B. Wilson, D/W. Moore, and B.S. Van Gosen, 2007, Preliminary integrated geologic map databases for the United States: Central States: Montana, Wyoming, Colorado, New Mexico, North Dakota, South Dakota, Nebraska, Kansas, Oklahoma, Texas, Iowa, Missouri, Arkansas, and Louisiana, *U.S. Geol. Survey Open File Report*, **OF 2005-1351**.

Swesnik, R.M. and T.H. Green, 1950, Geology of Eola Area, Garvin County, Oklahoma, *Bull. Amer. Assoc. Petrol. Geol.*, **34(11),** p 2176-2199.

Talwani, P. and S. Acree, Pore Pressure Diffusion and the Mechanism of Resevior-Induced Seismicity, *Pageoph*, **122**, p. 947-965.

Tanner, J.H. III, 1967, Wrench fault movements along Washita Valley fault, Arbuckle Mountain area, Oklahoma, *Bull. Amer. Assoc. Petrol. Geol.*, **51(1)**, p. 126-134.

Tryggvason, E., and B.R. Qualls, 1967, Seismic refraction measurements of crustal structure in Oklahoma, *J. Geoph. Res.*, **72(14),** 3738-3740.

Waldhauser, F. and W.L. Ellsworth, 2000, A double-difference earthquake location algorithm: Method and application to the northern Hayward fault, *Bull. Seismol. Soc. Am.,* **90**, 1353-1368.

Waldhauser, F., 2001, hypoDD: A Program to Compute Double-Difference Hypocenter Locations, *U.S. Geol. Survey Open File Report*, **OF 01-113**.